PCCP

Accepted Manuscript

This is an *Accepted Manuscript*, which has been through the Royal Society of Chemistry peer review process and has been accepted for publication.

Accepted Manuscripts are published online shortly after acceptance, before technical editing, formatting and proof reading. Using this free service, authors can make their results available to the community, in citable form, before we publish the edited article. We will replace this *Accepted Manuscript* with the edited and formatted *Advance Article* as soon as it is available.

You can find more information about *Accepted Manuscripts* in the **Information for Authors**.

Please note that technical editing may introduce minor changes to the text and/or graphics, which may alter content. The journal's standard **Terms & Conditions** and the **Ethical guidelines** still apply. In no event shall the Royal Society of Chemistry be held responsible for any errors or omissions in this *Accepted Manuscript* or any consequences arising from the use of any information it contains.

ROYAL SOCIETY OF CHEMISTRY

www.rsc.org/pccp

PCCP

ARTICLE

Ligand-exchange mechanism: new insight into solid-phase extraction of uranium based on a combined experimental and theoretical study

Yin Tian,[a,b] Jia Fu,[b] Yi Zhang,[b] Kecheng Cao,[a] Chiyao Bai,[a] Dongqi Wang,[d] Shoujian Li,*[a] Ying Xue,*[a] Lijian Ma*[a] and Chong Zheng*[c]

In numerous reports on selective solid-phase extraction (SPE) of uranium, the extraction of uranium is generally accepted as a direct coordination of the ligands on solid matrix with the uranyl, in which the critical effect of the hydration shell on the uranyl is neglected. The related mechanism in the extraction process remains unclear. Herein, the detailed calculation of activation energy and the geometry of the identified transition states reveal that the uranium extraction by a newly-synthesized urea-functionalized graphite oxide (Urea-GO) is in essence an exchange process between the ligands on Urea-GO and the coordinated water molecules in the first hydration shell of the uranyl. Moreover, we demonstrate that it is the ketone oxygen in the urea ligand to displace the coordinated water molecule of uranyl due to its stronger bonding ability and lower steric-hindrance, whereas the nitrogen atoms in the same ligand is proved to be an electron donor that enables the oxygen atom to have stronger affinity for uranium through electron delocalization effects evaluated on the basis of calculations of the second-order interaction energy between donor and acceptor orbitals. We therefore propose a new ligand-exchange mechanism for the SPE process. This study advance fundamental understanding of uranium extraction, and provide theoretical and practical guidance on ligand design for selective complexation of uranium(VI) and other metal ions in aqueous solution. Finally, the effect of nitrate ion on the extraction of uranyl was successfully explained based on the experimental and theoretical study.

Introduction

With increasing in environmental pollution and the depletion of fossil fuel reserves, nuclear energy, as a clean, safe, reliable and efficient source of energy, become more and more important to the sustainable energy supply.[1-4] Now, uranium is considered to be not only an important raw material of nuclear energy, but also a long-term potential environmental hazard because of its chemical and radiological toxicity.[4-6] So, separation and recovery of uranium from various uranium-containing aqueous systems, such as seawater, nuclear fuel effluents, mining effluents and others, have been a very active area of research, especially in recent years.[7,8]

The techniques applied to this area fall into two major types: liquid-liquid extraction (LLE), and solid-phase extraction (SPE). LLE is dominated by phosphorous-based extractants, such as the well-known tri-butyl-phosphate (TBP) and carbamoyl methyl phosphine oxides (CMPO).[9] And SPE is based mainly on nitrogen-based extractants predominantly including amide and amine functional groups.[8,10]

Since the beginning of the last century, thousands of research reports on various uranium selective solid-phase

extractants have emerged.[7,10-14] However, the detail of the extraction of uranium is still not fully understood. So the design and development of new SPE materials are largely a trial-and-error process until now. Many proposed structures and mechanisms for the extraction of uranium still remain questionable.

Recently, remarkable theoretical[15-24] and experimental[25-29] studies demonstrate that the interaction between the doubly charged uranyl cation and water molecules could result in a hydration sphere. The hydration sphere is composed of a first hydration shell with water molecules coordinated directly to the uranyl ion in the equatorial plane (about five water molecules), and a second hydration shell with a second group of water molecules associated through hydrogen bonding to the water molecules in the first hydration shell (about ten water molecules[15,16]). Correlation studies further stated that at different pH conditions, the coordination environment and the species of the uranyl ion could be changed, for example, $[UO_2(H_2O)_5]^{2+}$ at lower pH (pH < 3),[30,31] dimer $[(UO_2)_2(OH)_2(H_2O)_6]^{4+}$ and trimer $[(UO_2)_3(O)(OH)_3(H_2O)_6]^-$ as
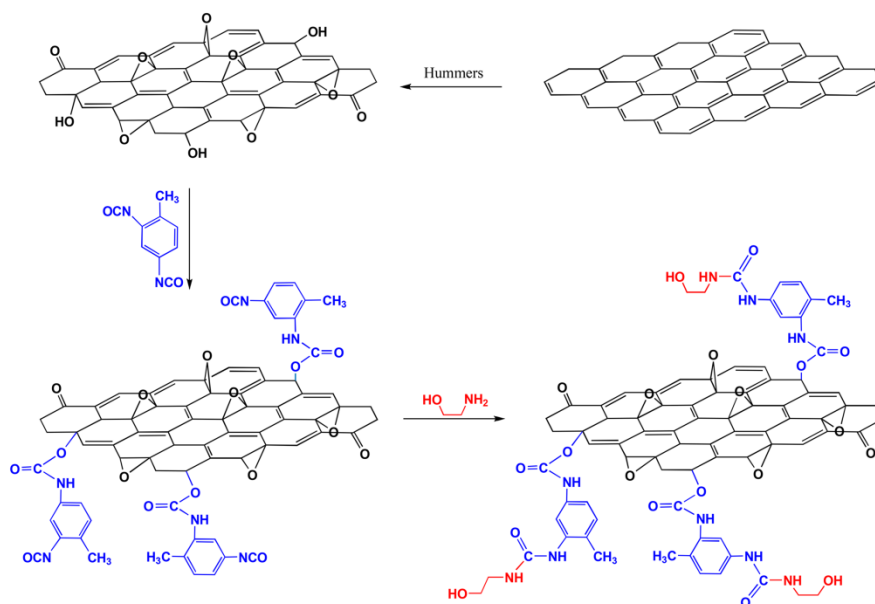
Fig. 1 A schematic description for in situ assembly of nitrogen-containing ligands onto graphite oxide platelets

the pH increases to about 4,[32–34] and $[UO_2(OH)_{4/5}]^{2-/3-}$ in highly alkaline solution (about pH = 12).[26,28,29,35]

Furthermore, the Wipff[36], Beck[37] and Khomami[38,39] groups studied the interaction between uranyl ion and the famous alkyl phosphate extractant (APE), typically TBP, used in the industrial-scale PUREX solvent extraction process for nuclear fuel reprocessing by molecular dynamics (MD) simulations. Very recently, MD simulations and density functional theory (DFT) calculation were also used by Wipff et al.[40] and Shi et al.[41], respectively, to study the extraction of the uranyl ions by CMPO, another APE, which is employed in TRUEX (transuranium extraction) process for separation of actinides from nuclear waste.

Up to now, almost all theoretical studies have focused mainly on APEs, which were mostly employed in uranium LLE processes at industrial scale. There is still much research that needs to be done to gain deeper insights into the mechanism of uranium SPE. Recently, DFT calculation was used by Shi et al. to study the structure of extraction complex for the uranium SPE by using graphene oxide.[42] Lin et al. reported their excellent works on a combined experimental and DFT study of the structure of extraction complex and reaction energy for SPE of uranium by CMPO-like structure functionalized metal-organic frameworks (MOF).[43] However, to the best of our knowledge, there have been no reports about a combined experimental and theoretical investigation of the reaction mechanism of uranium SPE.
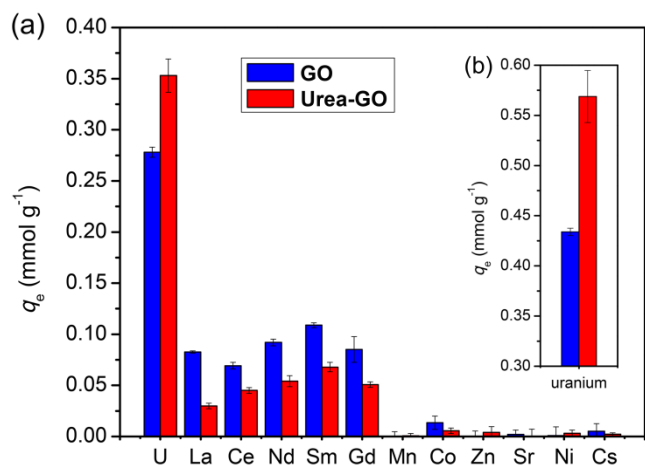
Herein, by using experimental and DFT methods, we studied the mechanism of uranium extraction by a urea-functionalized graphite oxide-based SPE material (Urea-GO) specifically designed and synthesized via an in situ "grafting-from" approach. Urea-GO is selected as the uranium-selective sorbent for the following reasons: 1. GO is an excellent solid matrix with larger specific surface area, relatively high thermal and radiation stability, high chemical resistance, especially in acidic medium, and harmless to the environment; 2. There are abundant hydroxyl groups on the surface of GO, which are conducive to further grafting of selected ligand; 3. The urea

ligand possesses double bond oxygen atom with structural similarity to APE; 4. Nitrogen atom in urea ligand is also regarded as an excellent donor atom to uranium. The sorption capacity of the as-synthesized Urea-GO towards uranium was investigated via batch sorption experiments in both single uranium solution and a simulated nuclear industry effluent sample containing 12 coexisting metal ions including uranyl ion. The mechanism of the interaction process between ligands on Urea-GO and uranyl ion in solution, thermodynamic function changes and also the coordination characteristics were studied systematically. And the research method used herein and the consequent results were further extended to the APE-like liquid phase extractants widely used in nuclear fuel reprocessing for the purpose of exploring a "universal" mechanism for the uranium extraction process.

Results and discussion
Preparation of SPE adsorbent and uranium(VI) extraction experiments

A two-step "grafting" procedure was employed for anchoring the urea structure onto the as-prepared GO lamellar matrix to develop a new SPE adsorbent (Urea-GO). A schematic description for Urea-GO synthesis is shown in Fig. 1 and the results of characterization are described in Electronic Supplementary Information (ESI) 1†. The extraction experiments were performed in both pure uranium(VI) solution and uranium-containing multi-ion system by using GO matrix and Urea-GO for comparison. The results about the effect of pH, temperature, extraction time and initial U(VI) concentration on the extraction of U(VI) by Urea-GO are given in ESI 5†. The results are shown in Fig. 2a. As expected, in the multi-ions system, the U(VI) adsorption capacity (q_{e-u}, see the Methods section) increased significantly from 0.27 mmol g^{-1} for GO to 0.35 mmol g^{-1} for Urea-GO, and the uranium selectivity (S_U, see Methods) also increased from 37.7% for GO to 57.3% for Urea-GO. A similar tendency was

2 | *Phys. Chem. Chem. Phys.*, 2015, **00**, 1-10

This journal is © The Royal Society of Chemistry 2015

Fig. 2 The uranium (VI) extraction experiments. (a) Adsorption capacity of coexistent ions on GO and Urea-GO (the initial concentrations c_0 = 0.50 mmol L^{-1} for all cations, pH = 4.5, all flasks shaking time t = 120 min, the volume of testing solution V = 25 mL, experiment temperatures T = 293 K, and the weight of adsorbent w = 10 mg). (b) the extraction experiments in pure uranium(VI) solution (the initial concentrations of uranyl ions c_0 = 0.50 mmol L^{-1}, pH = 4.5, t = 120 min, V = 20 mL, T = 293 K, w = 10 mg).

also observed in extraction experiments performed in the pure uranium (VI) solution (Fig. 2b). The results suggest that the functional groups or ligands such as urea grafted on Urea-GO possess stronger interaction ability with uranyl ion than those on GO.

Searching for the coordinating atoms

A combination of DFT calculations and X-ray photoelectron spectroscopy (XPS) measurements was employed to investigate the interaction between uranium and the ligands on the surface of Urea-GO. First, the coordination abilities of three possible coordinating atoms on the grafted component of Urea-GO: the hydroxyl oxygen atom, the ketone oxygen, and the nitrogen atom in the urea ligand, with uranyl hydrates ($[UO_2(H_2O)_5]^{2+}$) in aqueous medium were evaluated by the DFT calculations. The changes in enthalpy (ΔH), entropy (ΔS) and Gibbs free energy (ΔG) were listed in Table 1, and the relative free energy profiles are also presented in Fig. 3. As reported in Table 1, for coordination reaction of the ketone oxygen in urea, the ΔH and ΔG are −50.9 kJ mol^{-1} and −31.5 kJ mol^{-1}, respectively, suggesting that this process is spontaneous and exothermic. Conversely, for the other two coordinating atoms, the ΔH and ΔG are all positive. Moreover, the natural bond orbital (NBO) analysis was performed to analyze the Wiberg bond order values (WBOs) of the three extraction complexes (see Table S6 in ESI†). The structures of these complexes are shown in Fig. S6 in ESI†. The WBOs of the U–O (ketone oxygen) bond is 0.699, larger than those of the U–N and U–O (hydroxyl oxygen) bonds (0.340 and 0.442, respectively), which further indicates that the ketone oxygen in urea have stronger bonding ability towards uranyl ions than the other two atoms. As depicted in
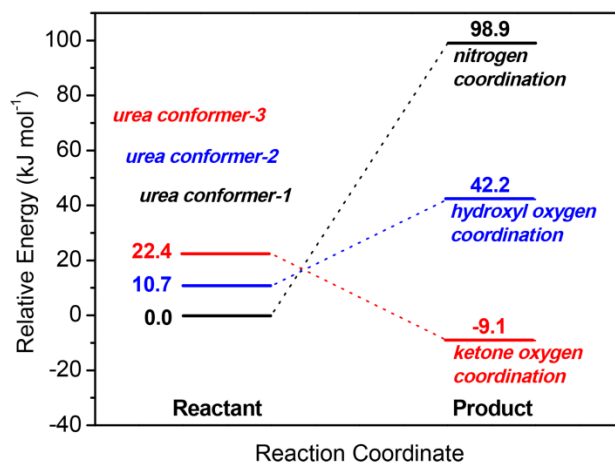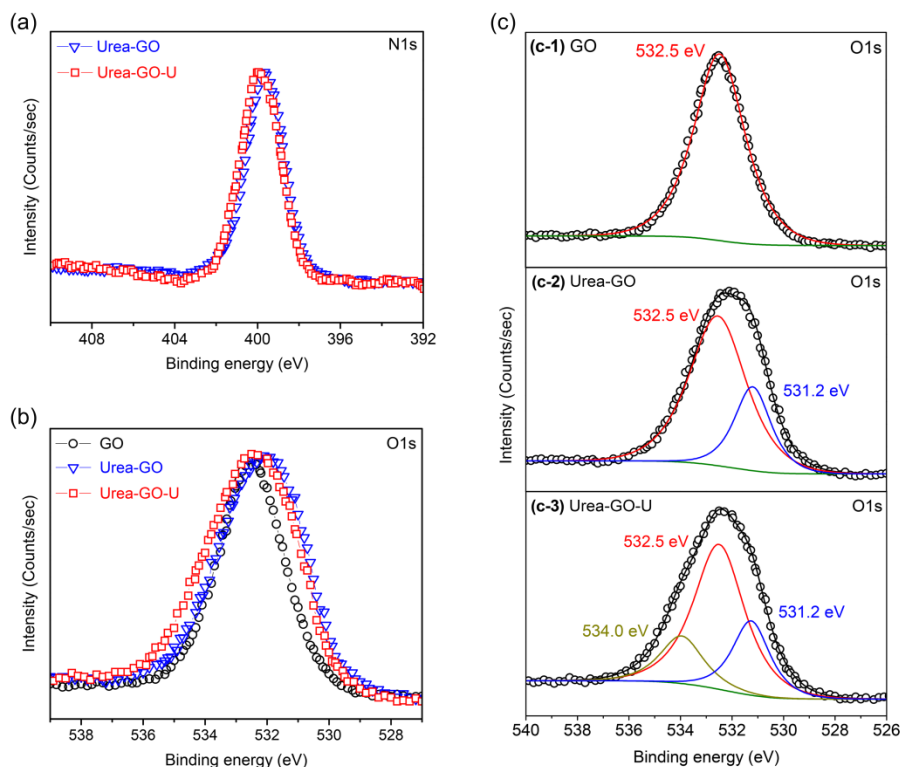

Fig. 3 Relative free energy profiles along the interaction between uranyl and the different coordinating atom of urea in aqueous solution obtained by the DFT calculations. The optimized structures of the stationary points are described in ESI† Fig. S6. (coordination reaction: $[UO_2(H_2O)_5]^{2+}$ + L → $[UO_2L(H_2O)_{5-x}]^{2+}$ + xH$_2$O, x = 1 for oxygen and x = 2 for nitrogen)

Table 1 DFT calculations of the ΔH (kJ mol^{-1}), ΔS (J mol^{-1} K^{-1}), and ΔG (kJ mol^{-1}) for the interaction between uranyl and the different coordinating atom including the nitrogen, the hydroxyl oxygen and the ketone oxygen atom on grafted component (urea structure) in aqueous solution.[a]

coordinating atom	ΔH	ΔS	ΔG
nitrogen	110.8	39.9	98.9
hydroxyl oxygen	11.8	−65.9	31.4
ketone oxygen	−50.9	−65.0	−31.5

[a]These values correspond to the structures in ESI†, Fig. S6.

Fig. 3, the relative free energy of ketone oxygen coordination product is the lowest, which corresponds to the most stable coordination structure. Meanwhile, for three urea conformers, only ΔG of ketone oxygen coordination product are all negative (−9.1 kJ mol^{-1}, the minimum one), which indicates that the formation of this product from any reactant conformers are spontaneous and exothermic processes. Furthermore, our theoretical analyses also reveal that the stable structure of the ligand will change accordingly during the coordinating process of nitrogen atom. That is, there is obvious steric hindrance on coordination of the nitrogen atom, which eventually leads to the positive ΔH and ΔG for the ligand-exchange reaction by the two donor nitrogen atoms (see ESI 3†, Table S7). The above results suggest that it should be only the ketone oxygen atom (O_L) to coordinate to the uranyl ion in the uranium extraction process. The nitrogen atom, which is generally believed to have stronger coordination ability, may not participate directly in the coordination as expected. Similarly, the X-ray absorption spectroscopy (XAS) experiments also demonstrate that it is the double bond oxygen atom (O_L) in APEs used in the industry scale PUREX process that will coordinate to the uranyl ion in the uranium extraction process.[44,45]

This journal is © The Royal Society of Chemistry 2015

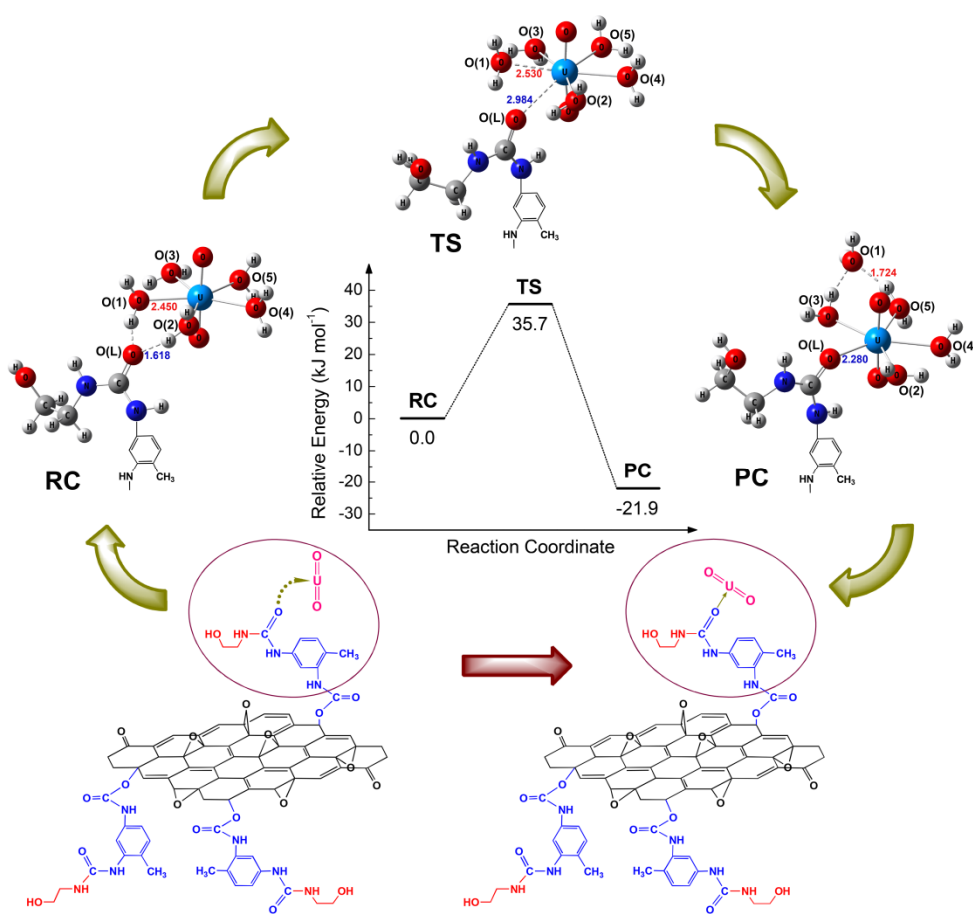*Phys. Chem. Chem. Phys.*, 2015, **00**, 1-10 | **3**

Fig. 4 The X-ray photoelectron spectroscopy of solid phase extractant GO and Urea-GO. (a) N 1s region of Urea-GO and after uranium sorption experiments Urea-GO-U. (b) O 1s region of GO, Urea-GO and Urea-GO-U. (c) the O 1s core-level spectra of GO (c-1), Urea-GO (c-2) and Urea-GO-U (c-3) are fitted with Gaussian-Lorentzian waveforms, which corresponds to the black lines, blue lines and red lines in (b), respectively.

XPS was used to investigate the changes in the chemical environment of the surface atoms and the surface chemical composition of the extractants. Fig. 4a shows N 1s binding energy of Urea-GO and Urea-GO-U (uranium-loaded Urea-GO). Fig. 4b displays O 1s binding energy of GO, Urea-GO and Urea-GO-U. In this work, O 1s core-level spectra are fitted with Gaussian-Lorentzian waveforms, and the results are presented in Fig. 4c. In Fig. 4c-1, the single absorbance peak at 532.5 eV is assigned to the C−OH (hydroxyl) and C−O−C (epoxide) groups, which indicates that epoxy and hydroxyl groups are main functional groups in GO. After chemical modification with urea ligand, O 1s peak became wider and moved toward lower binding energy (from black lines to blue lines in Fig. 4b), and splits into two peaks (Fig. 4c-2). The two new peaks occurring at 531.2 eV and 532.5 eV can be assigned to C=O (ketone), C−OH (hydroxyl) and C−O−C (epoxide) groups, respectively, which indicates that urea structure was successfully anchored onto the surface of GO nanosheets.[46,47] In Fig. 4b, after loading with uranium, O 1s peak of Urea-GO became wider and moved toward higher binding energy (from the blue lines to the red lines), and can be split into three peaks (Fig. 4c-3): The new signal at 534.0 eV corresponding to C=O−U was clearly observed.[48,49] This is because when the adsorption takes place, the adsorbed uranyl ions significantly decrease the electronic density around the ketone oxygen atom involved in the adsorption.[50] The second peak at 532.5 eV is also attributed to the C−OH (hydroxyl) and C−O−C (epoxide)

groups, and the peak at 531.2 eV is attributed to both the C=O group from the ligand on Urea-GO with no uranyl attached and that with the U=O group attached.[51−54] As can be seen in Fig. 4a, the N 1s spectra for Urea-GO were virtually identical before and after uranium sorption. (The XPS analysis for C 1s region and other results are shown in ESI† Fig. S3). Consequently, the coordinating atom on Urea-GO to uranyl is most likely the oxygen atom on the urea ligand, but not the nitrogen atom as conventionally thought. The results provided a strong evidence for the above DFT results.

The ligand-exchange mechanism

In light of the above findings, a new mechanism involving the interaction of the ligand on the SPE sorbent with uranyl ion in aqueous solution was proposed in more depth based on the DFT calculations. As shown in Fig. 5, this mechanism consists of the following steps: starting from the hydrogen-bonded reactant complex formed between the ligand and two water molecules in the first hydration shell of the uranyl ion, the nucleophilic oxygen atom (O_L) of the ligand attacks the electrophilic uranium atom, then one of the two water molecules is exchanged or replaced, and ultimately moves to the second hydration shell. In the transition states (TS), the imaginary frequency is $-66.81i$ cm^{-1}, which is mainly associated with the nucleophilic attack of the O_L atom to the uranium atom. As a

4 | *Phys. Chem. Chem. Phys.*, 2015, **00**, 1-10

This journal is © The Royal Society of Chemistry 2015

Fig. 5 Proposed ligand exchange mechanism of uranyl extraction based on our DFT calculation. First, the reactant complexes (RC), i.e., the uranyl hydrate, approaches to the coordinating oxygen atom (O_L) on GO to form two hydrogen bonds to two water molecules in the first hydration shell. Second, in the transition states (TS), the nucleophilic O_L attacks the electrophilic uranium atom, then one water molecule (corresponding to O(1)) moves to the second hydration shell. Third, in the product complexes (PC), a coordination bond is formed between O_L and the uranium atom. The potential energy profile for this process is depicted in the middle. The optimized structures of the stationary points are described in Fig. S7 in ESI†.
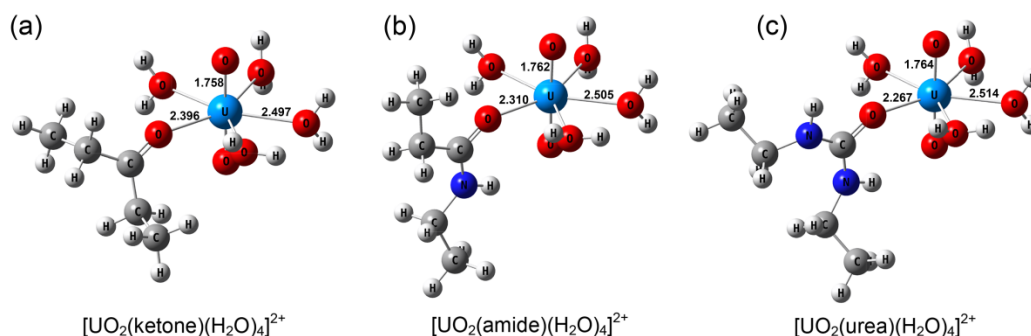
result in the NBO analysis (Table S10 in ESI†), the WBOs of the U–O_L bond is 0.686, much larger than that of the U–O (H_2O) bond (0.464), which indicates that the affinity of O_L to uranium is larger than that of H_2O. The detailed discussion about the WBOs for the various bond-breaking or bond-making processes is given in ESI 4.2†. The potential energy profiles for the interaction in aqueous solution are also presented in Fig. 5. It can be seen that the exchange between the urea ligand and the coordinated water molecule is an exothermic process with an activation energy barrier of 35.7 kJ mol^{-1}. The very low activation energy barrier could result in a very fast reaction rate.[55,56] The computational results are in line with the data of the kinetic experiment for the uranium adsorption in this study (see ESI 5.2† Fig. S14), which shows that over 65% of total adsorption amount was achieved in the first minute. Based on both the theoretical and experiment results, we hereby propose a "ligand exchange mechanism" for the uranium SPE process. The core of the extraction mechanism of uranium can be described as the exchange process between the ligand on solid-phase matrix and the coordinated water molecule in the first hydration shell of uranyl ion, and the prerequisite for the exchange is that the affinity or coordination ability of the ligand toward uranyl ions must be larger than that of water molecules.

Our DFT calculations also support a uranium extraction mechanism of the APEs similar to that described above (see ESI 4†). This is because of the similar ligand structure and coordinating atom. As depicted in Fig. S8 in ESI†, uranium extraction processes of urea and trimethyl phosphate (TMP, a representative sample of APEs) have nearly similar minimal energy path, indicating theoretically that the urea structure possesses nearly the same uranyl extraction ability as APE.

The role of nitrogen atom in urea ligand

In order to gain deeper insights into the ligand-exchange mechanism, we further studied the main factors affecting the exchange in the extraction by DFT. To explore the role of the

This journal is © The Royal Society of Chemistry 2015

Phys. Chem. Chem. Phys., 2015, **00**, 1-10 | **5**

Fig. 6 The role of nitrogen atom in the urea ligand. The optimized extraction structures of (a) the uranyl with ketone ($Et_2C=O$), (b) amide ((EtNH)EtC=O) and (c) urea ((EtNH)$_2$C=O) with the important bond lengths indicated.

Table 2 DFT calculations of changes in enthalpy(kJ mol^{-1}), entropy(J mol^{-1} K^{-1}), and Gibbs free energy (kJ mol^{-1}) for the complexing reactions of the three ligands with the uranyl, and the second order donor−acceptor interaction energy, $E^{(2)}$ (kJ mol^{-1}), for the n(N1) → π^* (C=O) interaction in amide (EtNH)EtC=O and urea (EtNH)$_2$C=O ligands in aqueous solution.^{a}

Ligand	ΔH	ΔS	ΔG	$E^{(2)}$ n(N1) → π^*(C–O)	$E^{(2)}$ n(N2) → π^*(C–O)
Et$_2$C=O	−2.1	−52.3	13.5		
(EtNH)EtC=O	−36.3	−32.8	−26.5	278.9	
(EtNH)$_2$C=O	−52.3	−52.4	−36.7	212.2	212.6

^{a}complexing reaction: [UO$_2$(H$_2$O)$_5$]$^{2+}$ + L → [UO$_2$(H$_2$O)$_4$L]$^{2+}$ + H$_2$O; And $E^{(2)}$ is given by $E^{(2)} = q_i(F_{i,j}^2)/(\varepsilon_j - \varepsilon_i)$ [79−81]

Table 3 Wiberg bond orders (WBOs) of various U–O bonds, natural charges on the coordinating oxygen atom before complexing Q(O$_L$), and changes in atom charges before and after complexing (ΔQ) in aqueous solution.^{a}

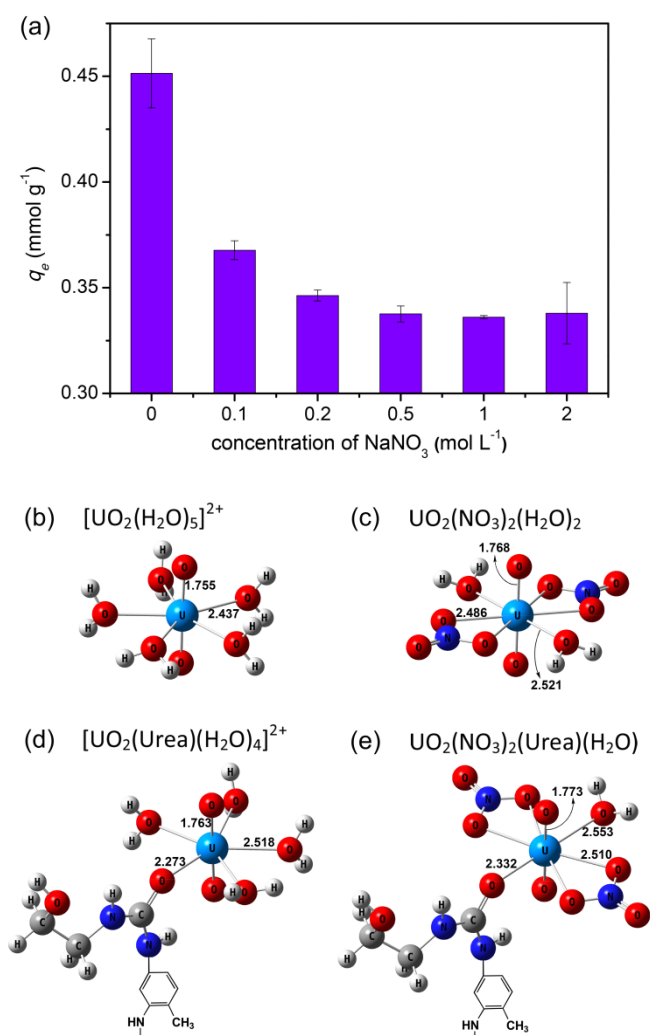| Ligand	Q(O$_L$)	ΔQ (O$_L$)	ΔQ (U)	U–O$_L$
Et$_2$C=O	−0.592	0.030	−0.045	0.504
(EtNH)EtC=O	−0.690	0.058	−0.081	0.630
(EtNH)$_2$C=O	−0.726	0.067	−0.102	0.709

^{a}the extraction structure of the stationary points are shown in Fig. 6

nitrogen atom in the urea ligand, we compared the uranium extraction ability of three ligands: urea ((MeN)$_2$C=O), amide ((MeN)EtC=O), and ketone (Et$_2$C=O), in which the number of nitrogen atoms decreased stepwise from 2 to 0. The ΔH, ΔS and ΔG for the extraction process of these three ligands in aqueous solution were calculated (Table 2). The WBOs and natural atomic charges (Q) were determined by NBO analysis (Table. 3), and the extraction structures are shown in Fig. 6. As described in Table 2, the order of the extraction capability for the three ligands is (MeN)$_2$C=O > (MeN)EtC=O > Et$_2$C=O. The ΔG for the Et$_2$C=O extraction process is positive. Moreover, the magnitude of WBOs of the U–O$_L$ bonds in three extraction complexes is also (MeN)$_2$C=O > (MeN)EtC=O > Et$_2$C=O (Table 3), which corresponds to the coordination ability toward uranyl. The charge distributions are shown in Table 3. From the analyses, we can qualitatively explain for the above trend: as the number of nitrogen atoms attached to carbon increases, the atomic charge at the coordinating oxygen (O$_L$) increases significantly from −0.592 for Et$_2$C=O to −0.727 for (MeN)$_2$C=O. The charge increase should lead to the increase of electrostatic interaction between the positively

charged U atom and negatively charged O$_L$ atom. Meanwhile, the magnitude of ΔG and ΔH for the three extractants also is determined by |ΔQ| (Table 3), defined as |Q(after adsorption)-Q(before adsorption)|,[57] because the more dispersion of the charge distributions at the extraction complex, the larger stability of the extraction complex. The above evidences demonstrate that the nitrogen atom in the urea ligand and also the amide ligand play only a role in providing the ketone oxygen atom with more negative charge and stronger bonding ability to uranyl. This is caused by electron delocalization effect in which the negative charge is transferred from the nitrogen lone pair to the π^*-orbital of C=O. The charge transfer can be evaluated by the second-order interaction energy between donor and acceptor orbitals, $E^{(2)}$, for n(N) → π^* (C=O) which are listed in Table 2. In addition, further DFT calculations found out that other soft atoms, such as phosphorus[36−41,58] and sulfur[59], will also enhance the bonding ability of the directly coordinated oxygen atom when they appear at appropriate locations (see ESI 4†).

Effect of nitrate concentration on the extraction of uranyl

On the other hand, uranium is generally extracted from concentrated nitric acid effluent generated during the nuclear fuel reprocessing cycle.[9,60,61] The effect of nitrate concentration on the uranium adsorption onto Urea-GO was experimentally investigated. As shown in Fig. 7(a), the adsorption amount of uranium(VI) on Urea-GO decreased significantly at first and then tended to be smoother gradually with increasing concentration of sodium nitrate. This phenomenon can be appropriately explained by our theoretical calculations. When nitrate ions exist in aqueous medium, the water molecules in the first hydration shell of uranyl will be exchanged by nitrate ions to form an UO$_2$(NO$_3$)$_2$(H$_2$O)$_2$

6 | *Phys. Chem. Chem. Phys.*, 2015, **00**, 1-10

This journal is © The Royal Society of Chemistry 2015

Table 4 DFT calculations of the ΔH (kJ mol^{-1}), ΔS (J mol^{-1} K^{-1}), and ΔG (kJ mol^{-1}) for the extraction reactions of $[UO_2(H_2O)_5]^{2+}$ and $UO_2(NO_3)_2(H_2O)_2$ by Urea.[a]

Adsorption species	ΔH	ΔS	ΔG
$[UO_2(H_2O)_5]^{2+}$	−50.87	−64.97	−31.50
$UO_2(NO_3)_2(H_2O)_2$	−35.44	−42.09	−22.89

[a]Extraction reaction: $[UO_2(H_2O)_5]^{2+}$ + urea → $[UO_2(urea)(H_2O)_4]^{2+}$ + H_2O and $UO_2(NO_3)_2(H_2O)_2$ + Urea → $UO_2(NO_3)_2(urea)(H_2O)$ + H_2O

Table 5 Wiberg bond orders (WBOs) of U–O bonds and selected atom charges (Q) in aqueous solution.[a]

species	U–O$_L$	U–O$_{water}$	Q(U)	Q(O$_L$)
$[UO_2(H_2O)_5]^{2+}$		0.433	1.802	
$UO_2(NO_3)_2(H_2O)_2$		0.410	1.477	
$[UO_2(urea)(H_2O)_4]^{2+}$	0.699	0.416	1.705	−0.655
$UO_2(NO_3)_2(urea)(H_2O)$	0.628	0.404	1.403	−0.635

[a]The structure are in Fig. 7, The optimized structures of the stationary points are depicted in ESI 4.3†.

Fig. 7 Effect of nitrate ions concentration on the extraction of U(VI). (a) The U(VI) extraction experiments by Urea-GO at different nitrate ions concentration (c_0 = 0.50 mmol L^{-1}, pH = 4.5, t = 120 min, V = 25 mL, T = 293 K, and w = 10 mg). The optimized structures of (b) $[UO_2(H_2O)_5]^{2+}$, (c) $(UO_2(NO_3)_2(H_2O)_2)$ in aqueous solution (CPCM). The structures of extraction complexes (d) $[UO_2(urea)(H_2O)_4]^{2+}$ and (e) $UO_2(NO_3)_2(Urea)(H_2O)$ (The optimized structures of the stationary points by DFT calculations are described in ESI 4.3†, Fig. S11).

structure[41,61,62] (see Fig. 7(b) and (c)). More details can be found in ESI 2†. It is worth mentioning that we found a lower energy conformer of $UO_2(NO_3)_2(H_2O)_2$ than the results of a similar research reported recently.[41] As shown in Table 4, the DFT calculations exhibit that the ΔG of the extraction reaction by urea is −22.9 kJ mol^{-1} in nitrate solution, but −31.5 kJ mol^{-1} in aqueous solution. The optimized extraction structure is described in Fig. 7(d) and (e). The decrease of $|\Delta G|$ in the above processes can also be qualitatively explained through the NBO analysis. The analysis of charge distribution and WBOs reported in Table 5 further reveals that the positive charges on the uranium atom in $UO_2(NO_3)_2(H_2O)_2$ are much smaller than those in $[UO_2(H_2O)_5]^{2+}$. Evidently the existence of nitrate ions directly leads to the weakening of the electrostatic interaction

between the positively charged U atoms and negatively charged O$_L$ atoms, which corresponds to the WBOs of the U–O$_L$ bonds in $[UO_2(urea)(H_2O)_4]^{2+}$ (0.699) and $UO_2(NO_3)_2(urea)(H_2O)$ (0.628), and accordingly resulted in the reduction of the amount of uranium adsorption. However, after almost all uranyl in solution transformed to $UO_2(NO_3)_2(H_2O)_2$ species, further addition of the nitrate ions will not influence the uranium adsorption. The results are in good agreement with the above experimental results (Fig. 7a). More remarkably, the theoretical calculations also indicate that the coordination ability of the nitrate ion to uranium is even stronger than O$_L$ atom in urea and also the oxygen doubly bonded to the P atoms in APE-like liquid-liquid extractants (see ESI† Table S2 and Table S15). It deserves noting, however, that in both the SPE and APE-like LLE, the two remaining water molecules in the first hydration shell of $UO_2(NO_3)_2(H_2O)_2$ are the species exchanged and displaced by the ligand atom on the extractants (see ESI 4.3†).[44,45]

Conclusions

In conclusion, selective extraction of uranium(VI) by the as-prepared Urea-GO as a typical case of metal separation by SPE approach has been investigated. Our combined experimental investigation and theoretical study demonstrated that the chemical nature of the uranium extraction is an exchange process between the donor oxygen atoms on the solid-phase ligand and the coordinated water molecules in the first hydration shell of uranyl ions. The positive role of the first hydration shell of uranyl ions on the extraction process is highlighted. Especially, the details of mechanism for the ligand interchange process have been clearly elucidated, and the "ligand-exchange mechanism" is therefore proposed for the first time. From this we obtain deeper fundamental understanding of the mechanism of SPE of uranium, which provides new theoretical and practical references for selection and design of the desired ligands with high-selectivity for uranium. Furthermore, the results of our DFT calculations for extraction of uranium(VI) by alkyl phosphate extractants (APE)

This journal is © The Royal Society of Chemistry 2015

Phys. Chem. Chem. Phys., 2015, **00**, 1-10 | **7**

indicated that the mechanism of APE-related liquid-liquid extraction is also the ligand-interchange reactions. And considering that selective extraction of uranium from aqueous system is now a very active branch of the field of metal ion separations, the proposed foundational mechanism can be extended to not only LLE for separation of uranium(VI), but also extraction of other aqueous metal cations based on both SPE and LLE approaches, which involving metal-ligand interaction. And moreover, similar to the case of the nitrogen atom in the urea ligand which endows the ketone oxygen atom in the same ligand with more negative charge and stronger bonding ability to uranyl, our DFT calculations suggest that other soft atoms, such as phosphorus[36–41,58] and sulfur[59,63], will also enhance the affinity of the coordinating oxygen for uranium when they appear at appropriate location.

Theoretical and experimental method

Quantum chemical calculations

All calculations were carried out with the hybrid B3LYP version[64,65] of the density functional method[66,67] by using Gaussian 09 program[68]. The Stuttgart quasirelativistic effective core potentials (RECPs) and their corresponding optimized basis sets were used to describe the uranium atoms.[69–71] The adopted small-core RECPs represents 60 core electrons in uranium. The 6-31G(d) basis set was used to describe phosphorus, oxygen, nitrogen, carbon and hydrogen atoms. The default fine grid (75, 302), having 75 radial shells and 302 angular points per shell, was used to evaluate the numerical integration accuracy. The geometric structures for all of the species were carried out in aqueous solution while employing the conductor-like polarized continuum model (CPCM)[72,73] with universal force field (UFF)[74,75] radii. For comparison, the gas phase (298.15 K, 0.1 MPa) structures of these species were also optimized in this work. The harmonic vibrational frequencies were also calculated after the geometry optimizations to characterize the nature of the stationary point as the true minimum with all positive frequencies, and the true transition state with only one imaginary frequency and to provide thermodynamic quantities such as the zero-point energy (ZPE), thermal correction, enthalpies (H), entropies (S) and Gibbs free energies (G). Next, the intrinsic reaction coordinate (IRC)[76,77] calculations were performed to verify the transition state (TS) associated with the correct reactant complexes (RC) and product complexes (PC). The natural atomic charges and Wiberg bond orders (WBOs)[78] were determined by natural bond orbital[79–81] analysis at the same level of theory.

Preparation of SPE sorbent (Urea-GO)

Graphite oxide (GO) was synthesized from natural graphite powder using the Hummers method[82] and dried in a vacuum desiccator. The isocyanate-modified GO (iGO) was prepared using the method reported by Stankovich et al.[83] In a typical procedure, 1g of GO was added to 50mL of anhydrous acetone. After ultrasonic dispersion, 5mL of toluene-2, 4-diisocyanate (TDI) was added to the mixture with stirring, then the mixture was refluxed under nitrogen for 24 h. The product was collected by centrifugation, washed with anhydrous acetone, and dried at 50 °C under vacuum. Next, 1g of iGO was added to 30mL of anhydrous acetone and then sonicated for 10 min, resulting in a suspension. Then, 2mL of ethanolamine (ETA) was added and the mixture was allowed to stir at room temperature for 24 h. The product Urea-GO was separated with centrifugation, washed with ethanol for at least 3 times, and dried at 50 °C under vacuum. The GO, iGO and Urea-GO were tested by Fourier transform infrared (FTIR) spectroscopy, elemental analysis (EA) and scanning electron microscope (SEM). The natural graphite powder, GO and Urea-GO were studied by X-ray diffraction (XRD). The GO, Urea-GO and Urea-GO-U (after loading with uranium) were characterized by XPS analysis.

Instrumental analyses

Powder XRD patterns of the products were obtained with a DX-1000 X-ray diffractometer (Dandong, China) using Cu Kα radiation (0.1542 nm) at 40 kV and 25 mA. XPS spectra were measured by XSAM800 X-ray photoelectron spectrometer (Kratos Ltd., UK). FT-IR spectra were plotted with a PerkinElmer IR-843 spectrometer (USA). EAs of the samples were performed on a Carlo-Erba 1106 elemental analyzer (Italy). The morphology of GO materials was examined by SEM (FEI Company, Oregon, USA). Inductively coupled plasma atomic emission spectroscopy (ICP-AES, Thermo Elemental, USA) was used to analyze the initial and equilibrium concentration of U(VI) (385.958 nm) and other metal ions (except for Cs^+) in the solution. Atomic adsorption spectroscopy (AAS, Beijing Haotianhui Science & Trade Co., Ltd., China) was used to determine the concentration of Cs^+ (852.607 nm).

The uranium(VI) extraction experiments

A certain amount of sorbent was added into a 50 mL Erlenmeyer flask along with 25 mL of uranium-containing multi-ion solution or pure uranium solution at given pH value. All the flasks were shaken for specified time (t) at desired temperatures (T). The concentrations of the metal ions, before and after adsorption, were determined. The adsorption amount (q_e, mmol g^{-1}) of metal ions were calculated by the equation $q_e = (c_0 - c_e)V/w$, where c_0 and c_e are the initial and equilibrium concentrations of metal ion (mmol L^{-1}), respectively, V is the volume of testing solution used for adsorption (L); and w is the weight of adsorbent (g). The uranium selectivity (S_U) is used to describe the potency and degree of the selectivity of the sorbents to uranium and is expressed by $S_U = q_{e\text{-}U}/q_{e\text{-}tot}$, where $q_{e\text{-}U}$ is the amount of uranium sorbed (mmol g^{-1}) and $q_{e\text{-}tot}$ is the amount of all cations sorbed (mmol g^{-1}) in multi-ion solution.

Abbreviations

8 | *Phys. Chem. Chem. Phys.*, 2015, **00**, 1-10

This journal is © The Royal Society of Chemistry 2015

SPE, solid-phase extraction; Urea-GO, urea-functionalized graphite oxide; DFT, density functional theory; LLE, liquid-liquid extraction; TBP, tri-butyl-phosphate; CMPO, carbamoyl methyl phosphine oxides; APE, alkyl phosphate extractant; MD, molecular dynamics; XPS, X-ray photo emission spectroscopy; NBO, natural bond orbital; WBOs, Wi-berg bond order values; XAS, X-ray absorption spectroscopy; RC, reactant complexes; TS, transition states; PC, product complexes; TMP, trimethyl phosphate; XRD, X-ray diffraction; FT-IR, Fourier transform infrared; EA, Elemental analysis; SEM, Scanning electron microscope.

Notes and references

a College of Chemistry, Sichuan University, Chengdu, 610064, People's Republic of China. E-mail: sjli000616@scu.edu.cn
b College of Physical Science and Technology, Sichuan University, Chengdu 610064, People's Republic of China. E-mail: megoborn@gmail.com
c Department of Chemistry and Biochemistry, Northern Illinois University, DeKalb, Illinois, 60115, USA. E-mail: cz1212@yahoo.com
d CAS Key Laboratory of Nuclear Radiation and Nuclear Energy Techniques, and Institute of High Energy Physics, Chinese Academy of Sciences, Beijing, 100049, China. E-mail: dwang@ihep.ac.cn

† Electronic Supplementary Information (ESI) available: Synthesis of graphite oxide (GO), SEM images, FTIR, XPS, XRD spectra, elemental analysis data, additional DFT calculation results, the optimized structures of the stationary points, and the detailed derivation of the site-adsorption model. See DOI: 10.1039/b000000x/

1   M. Z. Jacobson, *Energy Environ. Sci.*, 2009, **2**, 148.

2   R. Devanathan, L. V. Brutzel, A. Chartier, C. Guéneau, A. E. Mattsson, V. Tikare, T. Bartel, T. Besmann, M. Stan and P. V. Uffelen, *Energy Environ. Sci.*, 2010, **3**, 1406.

3   C. Degueldre, J. Bertsch, G. Kuri and M. Martin, *Energy Environ. Sci.*, 2011, **4**, 1651.

4   R. B. Silva, M. S. Kazimi and P. Hejzlar, *Energy Environ. Sci.*, 2010, **3**, 996.

5   T. P. Rao, P. Metilda and J. M. Gladis, *Talanta*, 2006, **68**, 1047.

6   M. W. Clark, J. J. Harrison, T. E. Payne, *J. Colloid Interface Sci.*, 2011, **356**, 699

7   Rao, L. *Recent International R&D Activities in the Extraction of Uranium from Seawater*; Lawrence Berkeley National Laboratory: Berkeley, CA, 2011, http://escholarship.org/uc/item/12h981cf.

8   J. Kim, C. Tsouris, R. T. Mayes, Y. Oyola, T. Saito, C. J. Janke, S. Dai, E. Schneider and D. Sachde, *Sep. Sci. Technol.*, 2013, **48**, 367.

9   K. L. Nash, R. E. Barrans, R. Chiarizia, M. L. Dietz, M. P. Jensen and P. G. Rickert, *Solvent Extr. Ion Exch.*, 2000, **18**, 605.

10   S. Sadeghi and E. Sheikhzadeh, *J. Hazard. Mater.*, 2009, **163**, 861.

11   T. E. Milja, K. P. Prathish, T. P. Rao, *J. Hazard. Mater.*, 2011, **188**, 384.

12   S. Sert and M. Eral, *J. Nucl. Mater.*, 2010, **406**, 285.

13   A. K. S. Deb, P. Ilaiyaraja, D. Ponraju and B. Venkatraman, *J. Radioanal. Nucl. Chem.*, 2012, **291**, 877.

14   Q. Song, L. Ma, J. Liu, C. Bai, J. Geng, H. Wang, B. Li, L. Wang and S. Li, *J. Colloid Interface Sci.*, 2012, **386**, 291.

15   P. Nichols, E. J. Bylaska, G. K. Schenter and W. de Jong, *J. Chem. Phys.*, 2008, **128**, 124507.

16   (a) G. A. Shamov and G. Schreckenbach, *J. Phys. Chem. A*, 2005, **109**, 10961. (b) G. A. Shamov and G. Schreckenbach, *J. Phys. Chem. A*, 2006, **110**, 12072

17   P. J. Hay, R. L. Martin and G. Schreckenbach, *J. Phys. Chem. A*, 2000, **104**, 6259.

18   L. Hemmingsen, P. Amara, E. Ansoborlo and M. J. Field, *J. Phys. Chem. A*, 2000, **104**, 4095.

19   S. Spencer, L. Gagliardi, N. C. Handy, A. G. Ioannou, C. K. Skylaris and A. Willetts, *J. Phys. Chem. A*, 1999, **103**, 1831.

20   S. Tsushima and A. Suzuki, *J. Mol. Struct. (THEOCHEM)*, 2000, **529**, 21.

21   B. Siboulet, C. J. Marsden and P. Vitorge, *Chem. Phys.*, 2006, **326**, 289.

22   M. Bühl, R. Diss and G. Wipff, *J. Am. Chem. Soc.*, 2005, **127**, 13506.

23   V. Vallet, U. Wahlgren, B. Schimmelpfennig, Z. Szabó and I. Grenthe, *J. Am. Chem. Soc.*, 2001, **123**, 11999.

24   V. Vallet, T. Privalov, U. Wahlgren and I. Grenthe, *J. Am. Chem. Soc.*, 2004, **126**, 7766.

25   L. Sémon, C. Boehme, I. Billard, C. Hennig, K. Lützenkirchen, T. Reich, A. Roßberg, I. Rossini and G. Wipff, *ChemPhysChem*, 2001, **2**, 591.

26   L. Soderholm, S. Skanthakumar and J. Neuefeind, *Anal. Bioanal. Chem.*, 2005, **383**, 48.

27   P. G. Allen, J. J. Bucher, D. K. Shuh, N. M. Edelstein and T. Reich *Inorg. Chem.*, 1997, **36**, 4676.

28   U. Wahlgren, H. Moll, I. Grenthe, B. Schimmelpfennig, L. Maron, V. Vallet and O. Gropen, *J. Phys. Chem. A*, 1999, **103**, 8257.

29   J. Neuefeind, L. Soderholm and S. Skanthakumar, *J. Phys. Chem. A*, 2004, **108**, 2733.

30   C. Nguyen-Trung, D. A. Palmer, G. M. Begun, C. Peiffert, R. E. Mesmer, *J. Sol. Chem.*, 2000, **29**, 101.

31   D. L. Clark, S. D. Conradson, R. J. Donohoe, D. W. Keogh, D. E. Morris, P. D. Palmer, R. D. Rogers and C. D. Tait, *Inorg. Chem.*, 1999, **38**, 1456.

32   S. Tsushima, A. Rossberg, A. Ikeda, K. Müller and A. C. Scheinost, *Inorg. Chem.*, 2007, **46**, 10819.

33   F. Quilès and A. Burneau, *Vib. Spectrosc.*, 2000, **23**, 231.

34   Y. Oda and A. Aoshima, *J. Nucl. Sci. Technol.*, 2002, **39**, 647.

35   J. Schreckenbach, P. J. Hay and R. L. Martin, *Inorg. Chem.*, 1998, **37**, 4442.

36   M. Baaden, R. Schurhammer and G. Wipff, *J. Phys. Chem. B*, 2002, **106**, 434.

37   M. Jayasinghe and T. L. Beck, *J. Phys. Chem. B*, 2009, **113**, 11662.

38   X. Ye, S. Cui, V. F. de Almeida and B. Khomami, *J. Phys. Chem. B*, 2009, **113**, 9852.

39   X. Ye, S. Cui, V. F. de Almeida, B. P. Hay and B. Khomami, *Phys. Chem. Chem. Phys.*, 2010, **12**, 15406.

40   A. Chaumont and G. Wipff, *Phys. Chem. Chem. Phys.*, 2006, **8**, 494.

41   C. Wang, J. Lan, Y. Zhao, Z. Chai, Y. Wei and W. Shi, *Inorg. Chem.*, 2013, **52**, 196.

42   Q. Wu, J. Lan, C. Wang, C. Xiao, Y. Zhao, Y. Wei, Z. Chai and W. Shi, *J. Phys. Chem. A*, 2014, **118**, 2149.

43   M. Carboni, C. W. Abney, S. Liu and W. Lin, *Chem. Sci.*, 2013, **4**, 2396.

44   C. Den Auwer, C. Lecouteux, M. C. Charbonnel, C. Madic and R. Guillaumont, *Polyhedron*, 1997, **16**, 2233.

This journal is © The Royal Society of Chemistry 2015

Phys. Chem. Chem. Phys., 2015, **00**, 1-10 | 9

45 C. Den Auwer, M. C. Charbonnel, M. T. Presson, C. Madic and R. Guillaumont, *Polyhedron*, 1998, **17**, 4507.

46 S. D. Gardner, C. S. K. Singamsetty, G. L. Booth and G. He, *Carbon*, 1995, **33**, 587.

47 K. Shimizu, C. Phanopoulos, R. Loenders, M. L. Abel and J. F. Watts, *Surf. Interface Anal.*, 2010, **42**, 1432.

48 A. N. Veleshko, E. V. Rumyantseva, I. E. Veleshko, A. Yu. Teterin, K. I. Maslakov, Yu. A. Teterin, S. A. Kulyukhin and G. A. Vikhoreva, *Radiochemistry*, 2008, **50**, 523.

49 A. N. Veleshko, I. E. Veleshko, A. Yu. Teterin, K. I. Maslakov, L. Vukčević, Y. A. Teterin and K. E. Ivanov, *Nucl. Technol. Radiat. Prot.*, 2008, **23**, 43.

50 X. Huang, X. Liao and B. Shi, *J. Hazard. Mater.*, 2009, **170**, 1141.

51 G. C. Allen, J. A. Crofts, M. T. Curtis, P. M. Tucker, D. Chadwick and P. J. Hampson, *J. Chem. Soc., Dalton Trans.*, 1974, 1296.

52 G. C. Allen, P. M. Tucker and J. W. Tyler, *J. Phys. Chem.*, 1982, **86**, 224.

53 D. L. Perry, L. Tsao and H. G. Brittain, *Inorg. Chem.*, 1984, **23**, 1232.

54 V. V. Atuchin and Z. Zhang, *J. Nucl. Mater.*, 2012, **420**, 222.

55 J. Gao, Y. Zeng, C. Zhang and Y. Xue, *J. Phys. Chem. A*, 2009, **113**, 325.

56 Z. Chen, C. Zhang and Xue Y., *J. Phys. Chem. B*, 2009, **113**, 10409.

57 X. Sun, X. Wei, X. Wu, Y. Ren, N. Wong and W. Li, *J. Phys. Chem. A*, 2010, **114**, 595.

58 M. Shamsipur, A. R. Ghiasvand and Y. Yamini, *Anal. Chem.*, 1999, **71**, 4892.

59 S. Sadeghi, D. Mohammadzadeh and Y. Yamini, *Anal. Bioanal. Chem.*, 2003, **375**, 698.

60 X. Ye, R. B. Smith, S. Cui, V. de Almeida and B. Khomami, *Solvent Extr. Ion Exch.*, 2010, **28**, 1.

61 M. Bühl, H. Kabrede, R. Diss and Wipff G. *J. Am. Chem. Soc.*, 2006, **128**, 6357.

62 J. S. Craw, M. A. Vincent and I. H. Hillier, *J. Phys. Chem.*, 1995, **99**, 10181.

63 M. J. Manos and M. G. Kanatzidis, *J. Am. Chem. Soc.*, 2012, **134**, 16441.

64 A. D. Becke, *J. Chem. Phys.*, 1993, **98**, 5648.

65 C. Lee, W. Yang and R. G. Parr, *Phys. Rev. B*, 1988, **37**, 785.

66 P. Hohenberg and W. Kohn, *Phys. Rev.*, 1964, **136**, B864.

67 W. Kohn and L. Sham, J. *Phys. Rev.*, 1965, **140**, A1133.

68 M. J. Frisch, *Gaussian 09*, Revision A.02, Gaussian, Inc.: Wallingford, CT, 2009.

69 W. Kuechle, M. Dolg, H. Stoll and H. Preuss, *J. Chem. Phys.*, 1994, **100**, 7535.

70 X. Cao, M. Dolg and H. Stoll, *J. Chem. Phys.*, 2003, **118**, 487.

71 X. Cao and M. Dolg, *J. Molec. Struct. (Theochem)*, 2004, **673**, 203.

72 V. Barone and M. Cossi, *J. Phys. Chem. A*, 1998, **102**, 1995.

73 M. Cossi, N. Rega, G. Scalmani and V. Barone, *J. Comput. Chem.*, 2003, **24**, 669.

74 S. Rayne and K. Forest, *J. Molec. Struct. (Theochem)*, 2010, **949**, 60.

75 S. Marque, V. Razafimahaléo, A. Dinut, G. Grach, D. Prim, X. Moreau and R. Gil, *New J. Chem.*, 2013, **37**, 2683.

76 K. Fukui, *J. Phys. Chem.*, 1970, **74**, 4161.

77 C. Gonzalez and H. B. Schlegel, *J. Chem. Phys.*, 1989, **90**, 2154.

78 K. B. Wiberg, *Tetrahedron*, 1968, **24**, 1083.

79 J. P. Foster and F. J. Weinhold, *J. Am. Chem. Soc.*, 1980, **102**, 7211.

80 A. E. Reed, R. B. Weinstock and F. Weinhold, *J. Chem. Phys.*, 1985, **83**, 735.

81 A. E. Reed, L. A. Curtiss and F. Weinhold, *Chem. Rev.*, 1988, **88**, 899.

82 W. Hummers and R. Offeman, *J. Am. Chem. Soc.*, 1958, **80**, 1339.

83 S. Stankovich, R. D. Piner, S. T. Nguyen and R. S. Ruoff, *Carbon*, 2006, **44**, 3342.

10 | *Phys. Chem. Chem. Phys.*, 2015, **00**, 1-10

This journal is © The Royal Society of Chemistry 2015